Journal of ELECTRONIC MATERIALS, Vol. 40, No. 7, 2011
DOI: 10.1007/s11664-011-1630-0

Numerical Modeling of the Performance of Thermal Interface Materials in the Form of Paste-Coated Sheets

PARISA POUR SHAHID SAEED ABADI[1,2] and D.D.L. CHUNG[1,3]

1.—Composite Materials Research Laboratory, University at Buffalo, State University of New York, Buffalo, NY 14260-4400, USA. 2.—*Present address:* George W. Woodruff School of Mechanical Engineering, Georgia Institute of Technology, Atlanta, GA 30332, USA. 3.—e-mail: ddlchung@buffalo.edu

The performance of thermal interface materials in the form of core sheets coated on both sides with a thermal paste is numerically modeled by finite-element analysis. The paste is polyol-ester-based carbon black paste and serves to improve the conformability. Good agreement is found between modeling and experimental results that involve copper proximate surfaces sandwiching the thermal interface material. The core sheets are copper, aluminum, indium, and flexible graphite. Flexible graphite (made from exfoliated graphite) is advantageous in its low elastic modulus, whereas copper and aluminum foils are advantageous in their high thermal conductivity. Indium is advantageous in its low elastic modulus compared with copper or aluminum and in its high thermal conductivity compared with flexible graphite. Among the four types of core sheet with identical thickness, coated indium foil gives the best performance for the range of foil thickness of 6 μm to 112 μm for the case of smooth (0.01 μm roughness) proximate surfaces and 117 μm to 320 μm for the case of rough (15 μm roughness) proximate surfaces. Aluminum foil gives the best performance for the thickness range of 112 μm to 2000 μm in the case of smooth proximate surfaces. For thicknesses below these ranges, flexible graphite performs the best. For thicknesses above these ranges, copper foil performs the best.

Key words: Thermal interface material, thermal gap-filling material, thermal paste, thermal contact conductance, finite-element modeling, carbon black

Nomenclature

q_x	heat flow rate in the x direction (W)
q_y	heat flow rate in the y direction (W)
k	thermal conductivity (W/m K)
A	area perpendicular to the heat flow direction (m^2)
T	temperature (K)
x, y	distance in the horizontal and vertical directions (m)
A_C	area of the 1 inch × 1 inch copper block (m^2)
k_C	thermal conductivity of copper (W/m K)
T_1, T_2, T_3, T_4	temperatures read by thermocouples 1 to 4 (K)
ΔT	temperature difference between T_1 and T_2 or between T_3 and T_4 (K)
T_A	temperature at the top surface of the thermal interface material (K)
T_D	temperature at the bottom surface of the thermal interface material (K)
d_A	distance between thermocouples T_1 and T_2 (i.e., 25 mm)
d_B	distance between thermocouple T_2 and the top surface of the thermal interface material (i.e., 5 mm)

(Received September 15, 2010; accepted March 16, 2011; published online April 23, 2011)

d_C	distance between thermocouples T_3 and T_4 (i.e., 25 mm)
d_A	distance between thermocouple T_3 and the bottom surface of the thermal interface material (i.e., 5 mm)
θ	thermal resistivity (m^2 K/W)
TCC	thermal contact conductance (W/m^2 K)

INTRODUCTION

As heat sink, heat spreader, heat pipe, Peltier, fluidic, and other methods of cooling improve, the bottleneck in heat dissipation shifts more and more toward interfaces, which tend to be associated with substantial thermal resistances. The thermal resistance of an interface can be decreased by the use of a thermal interface material (TIM).

In spite of the importance of TIMs, the science of TIMs is in its infancy. The relative importance of TIM attributes (e.g., thermal conductivity, conformability, spreadability, modulus, and viscosity) for the effectiveness of a TIM for various combinations of use conditions (e.g., clamping pressure and surface roughness) has received little prior attention. The widely accepted assumption is that the thermal conductivity is the most important TIM attribute. Due to this assumption, the thermal conductivity within the TIM is commonly taken as the performance descriptor of a TIM, and TIMs are formulated to contain ingredients with high thermal conductivity (e.g., silver, boron nitride, zinc oxide, and carbon nanotubes). Moreover, as the thermal conductivity increases with increasing content of the solid component, a high volume fraction of the solid component is commonly used (even though this impacts on conformability). However, recent work by Chung et al.[1–9] has shown that the above-mentioned assumption is not correct. Indeed, thermal pastes with high conformability but low thermal conductivity can perform as well as (or even better than) those of high thermal conductivity; for example, carbon black paste[2–6,8] is much more effective than carbon nanotube arrays.[10] In spite of the relatively high thermal conductivity of the carbon nanotube array, the large bond line thickness limits the effectiveness of the array as a TIM.[10] The importance of conformability is due to the need for the TIM to displace air from the interface by filling the microscopic valleys in the topography of the mating surfaces. The thermal conductivity becomes less important as the bond line thickness and the mating surface roughness decrease. This new understanding calls for a paradigm shift in the design of TIMs, brings to the front burner the need for understanding, characterizing, and controlling conformability (which is not the same as viscosity, due to the microscopic scale of the required conformability), and has given rise to thermal pastes that excel in conformability.

That the solid component does not have to be high in thermal conductivity or volume fraction widens the choice of solid components to include carbon black,[2–6,8] fumed alumina,[1] fumed zinc oxide,[1] nanoclay,[11] graphite nanoplatelets,[12] etc., and lowers the cost. Carbon black and fumed oxides are attractive in their being in the form of agglomerates of nanoparticles and the consequent squishability (conformability). Fumed oxides have the additional advantage of electrical nonconductivity. Nanoclay and graphite nanoplatelet are attractive in their almost single-atomic-layer thickness and the consequent small bond line thickness, which is advantageous for decreasing the thermal resistance. Graphite nanoplatelets have the additional advantage of substantial thermal conductivity. Both pastes that are electrically conductive (e.g., carbon black and graphite nanoplatelet pastes) and those that are electrically nonconductive (e.g., fumed oxide and nanoclay pastes) are addressed. Carbon black and fumed oxides are squishable, while their nanoparticles allow effective filling of the microscopic valleys in the mating surface topography. As a result, these pastes excel due to their conformability.

TIMs are commonly in the form of organic-based thermal pastes, e.g., polyol-ester-based pastes, with the organic component chosen by consideration of the fluidity, which relates to the conformability, and the thermal stability. Pressure perpendicular to the thermal interface helps conformability and consequently affects TIM performance. The effect of pressure also depends on the TIM modulus. Other use conditions include the proximate surface roughness and the bond line thickness.

The performance of a TIM should be evaluated when the TIM is sandwiched by selected surfaces, rather than being evaluated when the interface material is standing alone. The latter gives the thermal conductivity of the TIM itself. Although this thermal conductivity is a factor affecting the performance, it does not describe the performance of the material as a TIM.

The sandwich is a system that consists of the TIM and the two interfaces between the interface material and the two proximate surfaces. Each of these two interfaces is associated with a thermal resistance (referred to as the interfacial resistance), which can contribute significantly to the overall thermal resistance of the sandwich. The interfacial resistance depends on the nature of the interface as well as the area of this interface. This area is the true interface area that takes into account the area of the interface associated with the filled part of a valley in the surface topography. The true interface area increases with the fractional filling of the valleys. It is to be distinguished from the macroscopic geometric area of the thermal interface.

The performance of a TIM depends on the structure of the interface between the TIM and each of the two proximate surfaces, in addition to depending on the structure and thickness of the TIM. The structure of the interface depends on the surface roughness (particularly the typical height and width of the valleys in the surface topography) and the fractional filling of the valleys. The thickness of the TIM is often referred to as the bond line thickness. Thus, the ability of the TIM to be small in thickness is valuable. In the case of a thermal paste, this ability relates to the spreadability. The fractional filling of the valleys depends on the roughness of the surface, the pressure applied in the direction perpendicular to the interface for the purpose of squeezing the proximate surfaces together, and the elastic modulus, viscosity, and conformability of the TIM. A low modulus and a low viscosity improves spreadability. The higher the modulus, the greater the pressure required for the TIM to flow. In practical microelectronic applications, the pressure is limited. A low modulus and a low viscosity also help the conformability, but conformability requires not just the ability to flow macroscopically, but also the ability to fill microscopic valleys (even those on the nanoscale) in the surface topography. The filling of the valleys is necessary to displace air, which is thermally insulating, from the valleys. For the purpose of filling microscopic valleys, a microscopically structured (preferably nanostructured) interface material is valuable.

The relative importance of the various parameters mentioned above depends on the combination of their values. For example, the thermal conductivity of the TIM becomes more important as the thickness of the TIM increases and as the surface roughness (i.e., the height of the valleys in the surface topography) increases; the interfacial conductance (i.e., the reciprocal of the interfacial resistivity, which is the product of the interfacial resistance and the true interface area, with the interface referring to that between the TIM and one of the surfaces) becomes more important as the true interface area decreases.

The performance of a TIM is described by the thermal contact conductance (TCC, in units of W/m^2 K), which refers to the thermal conductance of the overall thermal contact in the direction perpendicular to the plane of the sandwich. This conductance is the reciprocal of the thermal contact resistivity (in units of m^2 K/W), which is the product of the total thermal resistance (in units of K/W, i.e., the temperature difference across the thermal contact divided by the heat power) of the thermal contact and the geometric area (in units of m^2) of the thermal interface. Due to the number and interdependence of the various parameters mentioned above in governing the TCC, a complete experimental investigation of all the parameters is difficult. Furthermore, it is difficult to obtain TIMs that cover a substantial range of each of the parameters (including thermal conductivity, modulus, viscosity, and conformability) for the purpose of systematic experimental evaluation. Therefore, understanding of the performance of TIMs requires modeling of this performance.

Abadi et al.[13] provided numerical thermal modeling of TIM performance for various combinations of TIM attributes and use conditions. Other prior work on modeling of TIM performance involved analytical models. Most commonly, such modeling is based on an equivalent circuit of the thermal resistances, which include those of the TIM and of the interface between the TIM and each of the two proximate surfaces.[14–18] The thermal resistance of this interface has been modeled by consideration of the degree of filling of the valleys in the surface topography.[14–16] In prior finite-element modeling (FEM), asperities on the surfaces of the proximate surfaces are not modeled and the interfacial resistance is indirectly modeled by using a TIM thermal conductivity value that is below the actual value.[17,19,20] Without modeling the asperities, evaluation of the effect of pressure, roughness, TIM thickness, TIM modulus, and interfacial conductance on the performance of the TIM is not possible. However, the complexity of the combination of geometric, thermal, mechanical, and material factors calls for numerical modeling.

TIM performance depends on a number of parameters, especially the surface roughness, TIM thickness, TIM thermal conductivity, TIM modulus, interfacial conductance of the surface–TIM interface, interfacial conductance of the surface–surface interface, and the applied pressure. Prior experimental work[1–12] addressed specific thermal interface materials without covering a substantial range of any parameter. Modeling work allows systematic evaluation of the effect of each of these parameters.[13]

Due to the substantial gap that needs to be filled by a thermal interface material in some applications, a thermal interface material may be in the form of a standalone sheet, which is ideally made of a material that is conformable and has high thermal conductivity. Such thermal interface materials are known as thermal gap-filling materials. Silicone-matrix composites containing thermally conductive fillers are common among gap-filling materials, due to the resiliency of the silicone matrix. In spite of this resiliency, the conformability is inadequate, thus causing poor performance. A thermally conductive sheet (e.g., aluminum foil, copper foil, and flexible graphite) that is coated on both sides with a highly conformable thermal paste (e.g., carbon black paste) has been shown to be more effective.[3] Flexible graphite, which is made by compression of exfoliated graphite flakes in the absence of a binder,[21] is resilient in the direction perpendicular to the sheet. In contrast, aluminum and copper foils are not as resilient as a flexible graphite sheet. In spite of this inherent difference among the sheets, the

effectiveness of such paste-coated sheets is comparable for these three types of sheet. This is because of the conformability provided by the thermal paste, the presence of which enhances the performance for each of the three types of sheet.[3] Due to its low melting point (156°C), indium is used as a thermal interface material in the form of a solder that is applied in the molten state.[22,23] Indium is softer than aluminum or copper, but is stiffer than flexible graphite.

This paper extends the numerical modeling work of Abadi et al.[13] from thermal pastes to thermal-paste-coated sheets. An objective is to understand the factors that govern the performance of TIMs in the form of thermal-paste-coated sheets. Another objective is to investigate by modeling the effect of the thickness of the sheet, for a thickness range much beyond what has been investigated experimentally.[3] Furthermore, the performance of indium foil as a core sheet is evaluated. The understanding provided by the modeling will aid the future design and development of thermal gap-filling materials.

MODELING METHODOLOGY

The finite-element modeling is conducted using commercial ANSYS software. Modeling all the complications of a three-dimensional (3-D) surface would require extensive computational effort. Furthermore, different areas of a surface differ in their topography. Therefore, a two-dimensional (2-D) model of a single asperity of the surface with the average roughness of the surface is employed in this work. The 2-D model has resulted in reasonable results in previous work.[13]

It is assumed that no heat loss to the environment occurs. Heat transfer due to radiation and natural convection is negligible compared with conduction through the contact points, due to the moderate range of temperature and the small size of the air gaps at the thermal interface.

The surface roughness is modeled as consisting of an arc, such that the arcs of the two proximate surfaces are aligned, with the bottom point of a hillock of the upper surface aligned with the top point of a hillock of the lower surface, as illustrated in Fig. 1. The dimensions and boundary temperatures in Fig. 1 are presented in Table I. This model considers only the bottom portion of the upper copper block and the top portion of the lower copper block. These hillock shapes are used because they roughly represent the actual situation and are similar to the hemispherical hillocks used in 3-D contact models in prior analytical work.[24,25]

Table I presents the dimensions of the overall TIM, which includes both the core sheet and the coating on both sides of the sheet. Table II presents the dimensions of the coating and the core sheets separately. The coating is carbon black thermal paste with polyol ester as the vehicle.[4] It is identical in composition and thickness on the two opposite

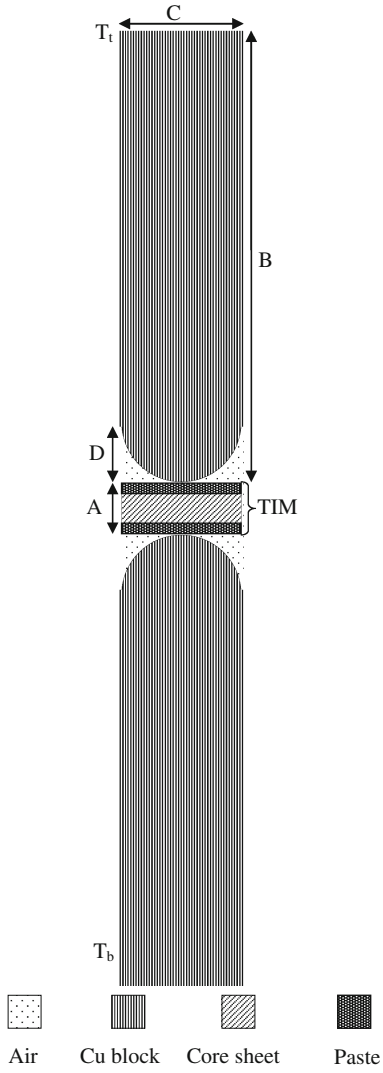

Fig. 1. The thermal contact structure used in the modeling. The dimensions indicated in Table I are used.

sides of the sheet. Four types of sheet are modeled, namely copper foil, aluminum foil, indium foil, and flexible graphite. The thickness, elastic modulus, and thermal conductivity of these four material components are listed in Table II. The paste thickness is 0.4 μm in the case of rough copper proximate surfaces (15 μm roughness) and 0.2 μm in the case of smooth copper proximate surfaces (0.01 μm roughness), as based on experimental values.[1–3,11,26] The dimensions presented in Tables I and II were used in the modeling. During the formation of the thermal contact, the TIM enters the valleys to a degree that depends on the combination of pressure and the TIM modulus.

All of the stages prior to pressure application cannot be modeled because of limited information available on the nonlinear behavior of the pastes. Therefore, the final geometry after applying pressure is modeled. The final geometry predicted (based on experimental results on the bond line

Table I. Dimensions in Fig. 1

Sheet	Proximate Surfaces	A (μm)	B (μm)	C (μm)	D (μm)	T_t (°C)[a]	T_b (°C)[b]
Aluminum	Rough	7.4	150	30	15	35.66	34.68
Aluminum	Smooth	7.2	150	30	0.01	35.66	34.68
Copper	Rough	13.4	150	30	15	35.66	34.68
Copper	Smooth	13.2	150	30	0.01	35.66	34.68
Flexible graphite	Rough	130.4	150	30	15	35.66	34.68
Flexible graphite	Smooth	130.2	150	30	0.01	35.66	34.68
Indium	Rough	7.4	150	30	15	35.66	34.68
Indium	Smooth	7.2	150	30	0.01	35.66	34.68

[a]Temperature at the top boundary of Fig. 1; [b]Temperature at the bottom boundary of Fig. 1.

Table II. Properties and thickness of TIM component materials

Material	Elastic Modulus[27,28] (GPa)	Thermal Conductivity[26–28] (W/m K)	Thickness (μm)
Aluminum core sheet	70	250	7
Copper core sheet	115	391	13
Indium core sheet	11	70	7
Flexible graphite core sheet	1.4	140[a] 5[b]	130
Carbon black paste	–	0.13	0.2[c] 0.4[d]

[a]In-plane direction; [b]Out-of-plane direction; [c]Smooth proximate surfaces; [d]Rough proximate surfaces.

thickness[11,26]) and modeled affects the calculated thermal contact conductance. Previous stages, before this final state, do not affect the final results.

In the case of rough copper surfaces, no change of bond line thickness was observed experimentally[26] for the carbon black paste (in the absence of a core sheet) with increasing pressure in the range of 0.46 MPa to 0.92 MPa. However, the measured TCC increased with increasing pressure, independent of whether the core sheet was present with the carbon black paste or not.[3,4] Based on these experimental results on the effect of pressure, we assume in this modeling that direct contact between the copper blocks and the core sheet occurs upon deformation of the paste. In the previously addressed case of the thermal paste without a core sheet,[13] contact between the two hillocks occurred when carbon black paste was modeled and did not occur when metal particle paste, with higher modulus, was modeled.

The initial conditions specified in the model are the thickness of the TIM, the temperature (T_b in Fig. 1) at the bottom surface of the modeled top portion of the lower copper block, and the temperature (T_t in Fig. 1) at the top surface of the modeled bottom portion of the upper copper block. The temperature T_t is calculated from the temperature gradient (0.093°C/mm, as in the experiment[1]) and T_b. However, according to the definition of the thermal contact conductance (the heat flux divided by the temperature difference across the thermal contact), the results are independent of the selected values of T_b and T_t. This independence is because both the temperature difference across the thermal contact and the heat power similarly depend on the difference between T_b and T_t, so that the quotient is independent of this quantity.

The sides of the geometry in Fig. 1 are assumed to be thermally insulated. Thermal expansion is ignored. The mechanical boundary condition is such that the bottom block is fixed in position. Upon the application of pressure in the direction perpendicular to the thermal contact, a part of the TIM enters the valleys and eventually achieves a steady state (final state), which is the state described by the results reported here.

The extent of filling of a valley can be calculated from the valley geometry and half of the displacement of the proximate copper surfaces relative to one another. The factor of half is due to the fact that filling occurs at the valleys of both copper blocks simultaneously. The displacement here is the entire displacement of one copper block relative to the other. The values of the fractional valley filling of the proximate surfaces in the previous work for the case of carbon black paste in the absence of a core sheet[13] are identical to those of this work for the case of the same paste in the presence of a core sheet. This similarity of the fractional valley filling

Table III. Values of the interfacial conductance for the interface between carbon black paste and core sheet and the interface between carbon black paste and copper block

Component Contacting the Paste	Interfacial Conductance (10^4 W/m^2 K)
Copper[a]	105
Copper[b]	18
Aluminum[b]	22
Indium[b]	26
Flexible graphite[b]	30

[a]Block; [b]Core sheet.

of the proximate surfaces for the cases with and without a core sheet is due to the high modulus of the core sheet compared with the paste.

The values of the interfacial conductance used in this model are listed in Table III. The value for the interface between the copper block and the paste is the same as the one used in the previous model of the carbon black paste.[13] The values for the interface between aluminum and the paste and for the interface between flexible graphite and the paste were calculated semi-empirically using the available TCC experimental values[3] and the finite-element model. This method is similar to the method used in the previous model for calculating the interfacial conductance between the paste and the copper block.[13] The difference is that, in the previous work, only one interfacial conductance was involved whereas here two interfacial conductances are involved, one between the copper block and the paste and the other between the paste and the core sheet. Using the value of the interfacial conductance between the copper block and the paste from the previous work,[13] the only unknown is the interfacial conductance between the core sheet and the paste, which can be calculated. The fact that, for both rough and smooth cases (with two different geometries), the TCCs calculated using these values of the interfacial conductance are close to the experimental values shows the acceptability of the selected values of the interfacial conductance. The values for the indium–paste interface and the copper–paste interface are selected with consideration of the experimental results for copper coated with polyethyleneglycol-based carbon black paste[3] and with consideration of the expected dependence of the interfacial conductance on the modulus of the core sheet. There is a substantial difference between the copper core sheet–paste interfacial conductance value (18×10^4 W/m^2 K) and the copper block–paste interfacial conductance of our previous work (105×10^4 W/m^2 K).[13] The reason that, for the copper core sheet and all other core sheets studied, the interfacial conductance is much lower than that for a copper block is due to the inevitable occurrence of wrinkles and other deformation of the core sheets, which are relatively thin. Since the core sheets are modeled as perfectly flat and smooth surfaces, any effect of the wrinkles and other deformation of the core sheets would appear in the calculated interfacial conductance values.

Due to the geometric symmetry (Fig. 1), only the left half of Fig. 1 is modeled, as shown in Fig. 2. This modeling involves the application of symmetric thermal and structural boundary conditions on the right edge of each model shown in Fig. 2. The finite-element mesh is shown in Figs. 2 and 3 for the case of rough and smooth copper surfaces, respectively. Each mesh is particularly dense in the vicinity of the interface between the paste and a copper proximate surface. Magnified views of parts of the dense regions are shown in Fig. 4. ANSYS elements PLANE223 (2-D eight-node coupled-field solid), CONTA172 (2-D three-node surface-to-surface contact), and TARGE169 (2-D target segment) are used. The element side length varies from 1.0 μm to 1.5 μm in the areas far from the contact area to 0.01 μm to 0.10 μm near the contact area. A convergence test was done by reducing the size of the elements to the point where no significant change in the results was observed on further mesh refinement, allowing the element size to be chosen.

In calculating the 2-D temperature distribution by finite element analysis, the following equations are used:

$$q_x = kA\frac{dT}{dx}, \tag{1}$$

$$q_y = kA\frac{dT}{dy}, \tag{2}$$

where x and y are the coordinates in the horizontal and vertical directions, q_x and q_y are the heat flow rates in the x and y directions across the cross-sectional area A perpendicular to the heat flow direction, k is the thermal conductivity of the medium, which is copper, air, or TIM, depending on the location; k is not a variable in the modeling work; T is the temperature. The heat diffusion equation for the case of 2-D steady-state heat flow in the absence of heat generation is

$$\frac{\partial}{\partial x}\left(k\frac{\partial T}{\partial x}\right) + \frac{\partial}{\partial y}\left(k\frac{\partial T}{\partial y}\right) = 0. \tag{3}$$

The modulus and pressure are two parameters that greatly affect the thermal contact conductance. This is mainly because of their effects on the contact area. A lower modulus and a higher pressure will result in a larger contact area, as in the case of the carbon black paste without a core sheet,[13] thereby leading to a higher thermal contact conductance. Furthermore, a higher pressure can result in a lower TIM thickness. In the modeling work, the

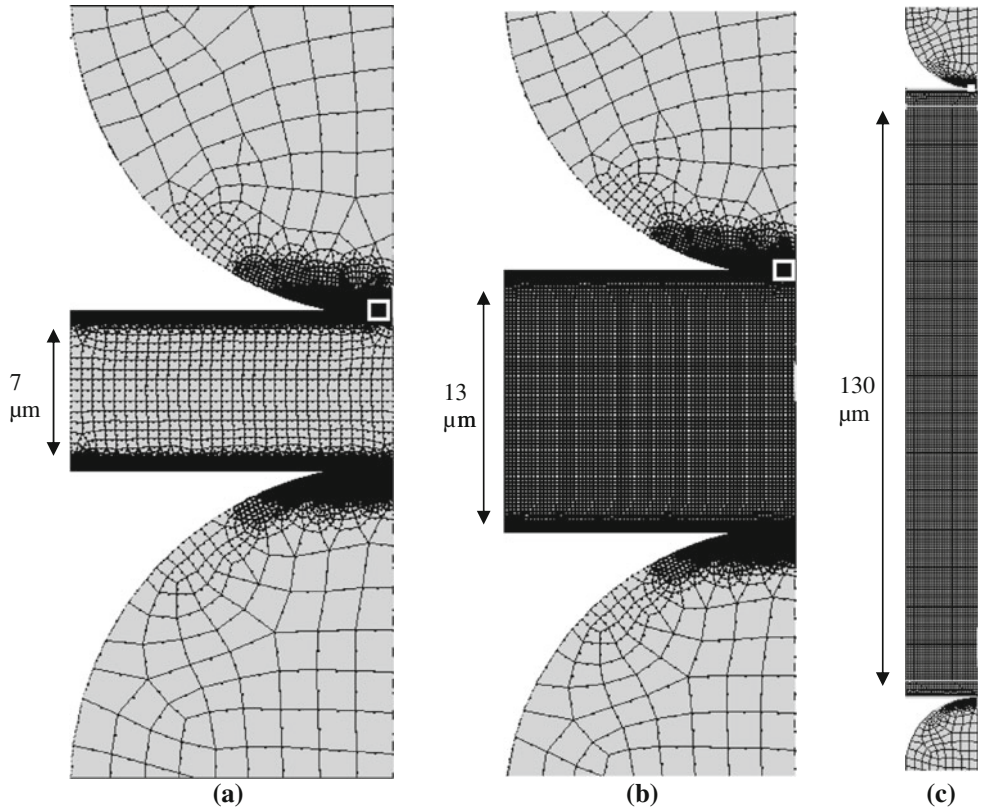

Fig. 2. Finite-element mesh for the case of rough proximate surfaces. (a) Aluminum or indium core sheet. (b) Copper core sheet. (c) Flexible graphite core sheet.

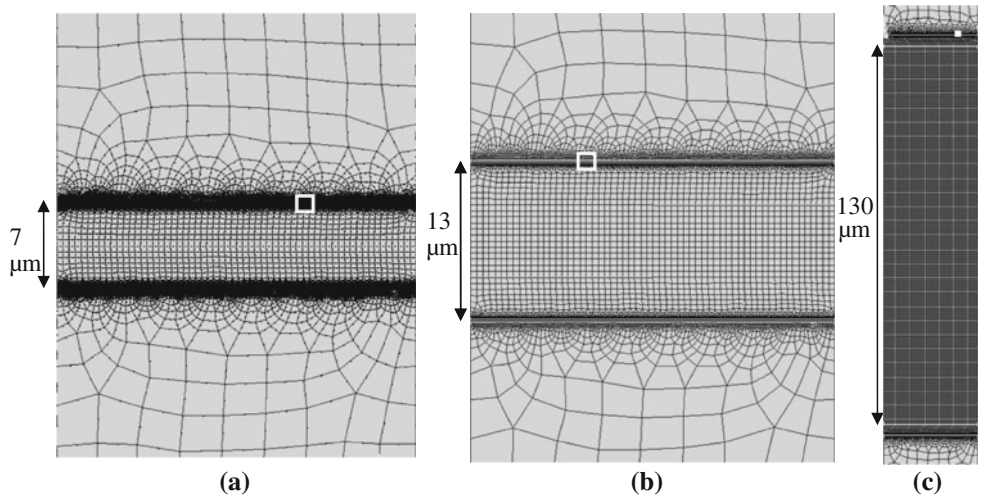

Fig. 3. Finite-element mesh for the case of smooth proximate surfaces. (a) Aluminum or indium core sheet. (b) Copper core sheet. (c) Flexible graphite core sheet.

modulus and pressure influence the outcome by affecting the dimensions.

The unfilled portion of each valley is filled with air. The thermal conductivity of air (0.026 W/m K to 0.028 W/m K)[18] is low compared with that of the paste (0.13 W/m K)[26] or that of the core sheet (5 W/m K to 390 W/m K).[3] Therefore, the areas which are in contact with air can be assumed to be thermally insulated, as is done in this modeling. The thermal conductivity of copper is 391 W/m K,[17] and the elastic modulus of copper is 115 GPa.[17]

The experimental results used in this work for comparison with the modeling results were obtained in prior work[3] using the method described below.

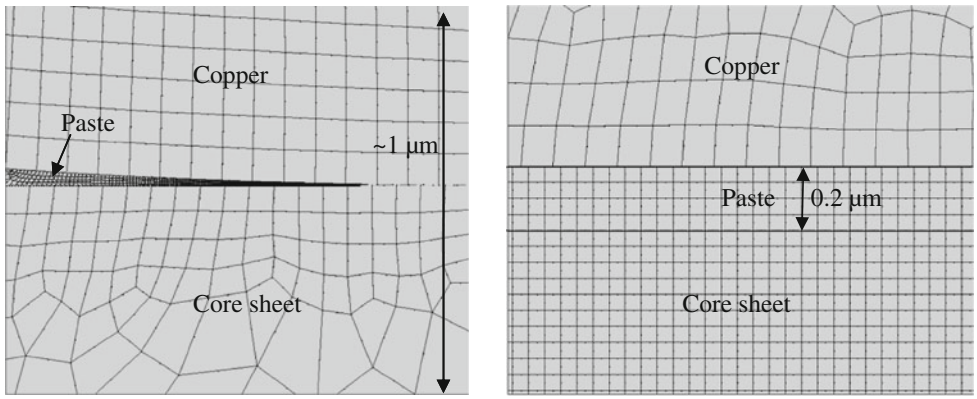

Fig. 4. Magnified finite-element mesh. (a) Magnified view of any of the three boxed areas with white outlines of Fig. 2, for the case of rough proximate surfaces. (b) Magnified view of any of the three boxed areas of Fig. 3, for the case of smooth proximate surfaces.

The TCC between two 1 inch × 1 inch (25 mm × 25 mm) copper blocks with a thermal interface material between them was measured using the guarded hot-plate method, which is a steady-state method of heat flux measurement (ASTM method D5470). During the period of temperature rise, the heating rate was controlled at 3.2°C/min by using a temperature controller. Heating was provided by heating coils, while cooling was provided by running water. The two mating surfaces of the two 1 inch × 1 inch copper blocks were either "rough" (15 μm roughness, as attained by mechanical polishing) or "smooth" (0.009 μm roughness and 0.040 μm to 0.116 μm flatness, as attained by diamond turning). Four thermocouples (type T) were inserted in four holes (T_1, T_2, T_3, and T_4 in Fig. 5, each hole of diameter 2.4 mm). Two of the four holes were in each of the 1 inch × 1 inch copper blocks. The temperature gradient was determined from $T_1 - T_2$ and $T_3 - T_4$. These two quantities should be equal at equilibrium, which was attained after holding the temperature of the heater at the desired value for 30 min. Equilibrium was assumed to have been reached when the temperature variation was within ±0.1°C for a period of 15 min. The pressure in the direction perpendicular to the plane of the thermal interface was controlled by using a hydraulic press at pressures of 0.46 MPa, 0.69 MPa, and 0.92 MPa.

In accordance with ASTM method D5470, the heat flow q is given by

$$q = \frac{k_C A_C}{d_A} \Delta T, \tag{4}$$

where $\Delta T = T_1 - T_2 = T_3 - T_4$, k_C is the thermal conductivity of copper, A_C is the area of the 1 inch × 1 inch copper block, and d_A is the distance between thermocouples T_1 and T_2 (i.e., 25 mm).

The temperature at the top surface of the thermal interface material is T_A, which is given by

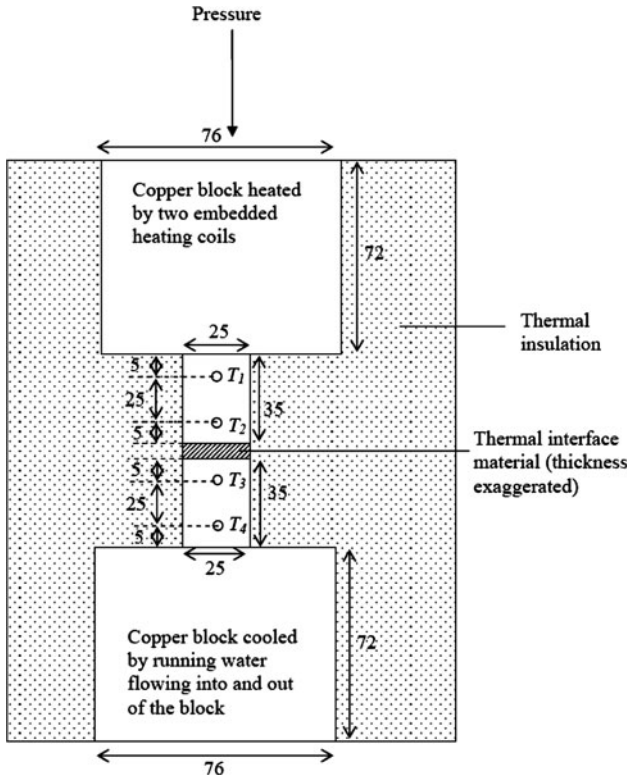

Fig. 5. Experimental setup for the guarded hot-plate method of thermal contact conductance measurement. T_1, T_2, T_3, and T_4 are temperatures measured by thermocouples (type T) inserted in each hole of diameter 2.4 mm. All dimensions are in mm.

$$T_A = T_2 - \frac{d_B}{d_A}(T_1 - T_2), \tag{5}$$

where d_B is the distance between thermocouple T_2 and the top surface of the thermal interface material (i.e., 5 mm). The temperature at the bottom surface of the thermal interface material is T_D, which is given by

Table IV. Thermal contact conductance (TCC) for various combinations of core sheet and proximate surface roughness

Roughness			Rough (15 μm)			Smooth (0.01 μm)		
Pressure (MPa)			0.46	0.69	0.92	0.46	0.69	0.92
TCC (10^4 W/m^2 K)	A	Modeling result	2.76	3.25	3.41	6.95	7.26	7.43
		Experimental result[3]	3.54 ± 0.30	3.85 ± 0.31	4.19 ± 0.37	6.22 ± 0.54	6.94 ± 0.61	7.09 ± 0.55
		Deviation (%)	22	15	19	12	5	5
	B	Modeling result	2.66	2.98	3.34	2.63	2.67	2.69
		Experimental result[3]	2.34 ± 0.16	2.60 ± 0.19	2.94 ± 0.24	3.09 ± 0.16	3.21 ± 0.27	3.48 ± 0.29
		Deviation (%)	14	15	14	15	17	23
	C	Modeling result	–	2.15	–	–	6.08	–
	D	Modeling result	–	3.68	–	–	7.87	–

Experimental results are not available for C and D. The deviation refers to the fractional deviation of the modeling result from the corresponding experimental result. A: coated aluminum foil; B: coated flexible graphite; C: coated copper foil; D: coated indium foil.

$$T_D = T_3 + \frac{d_D}{d_C}(T_3 - T_4), \tag{6}$$

where d_D is the distance between thermocouple T_3 and the bottom surface of the thermal interface material (i.e., 5 mm) and d_C is the distance between thermocouples T_3 and T_4 (i.e., 25 mm).

The thermal resistivity θ is given by

$$\theta = (T_A - T_D)\frac{A_C}{q}. \tag{7}$$

Note that insertion of Eq. (4) into Eq. (7) causes cancelation of the term A_C, so that θ is independent of A. The thermal contact conductance (TCC) is the reciprocal of θ.

RESULTS AND DISCUSSION

The modeling results are presented below for all four types of sheets (copper, aluminum, indium, and flexible graphite) with carbon black paste as the coating. The calculated TCCs for coated aluminum foil and coated flexible graphite for both the rough and smooth cases are compared with the corresponding experimental results.[3] No experimental results are available for coated indium foil or for copper foil coated with this particular type of carbon black paste. Nevertheless, the calculated TCCs have been obtained.

Table IV shows good agreement between modeling and experimental results for the coated aluminum foil and coated flexible graphite in both the smooth and rough cases. The deviation of the numerical results from the experimental results ranges from 5% to 22% and is mainly due to the difference between real surface asperities and the simplified 2-D asperity in our model. Considering the difficulty of modeling all 3-D surface details and also the difference between one rough surface and another, this range of deviation of the numerical values from the experimental values shows that the numerical values are reasonable enough to be used for explaining the difference between the performance of various materials and also for evaluating the performance of new materials. The calculated TCCs for coated copper foil and coated indium foil for both smooth and rough cases are also presented in Table IV.

In the rough case, the TCCs are comparable for the four types of coated sheets. Compared with flexible graphite, copper foil is disadvantageous in its high modulus, but it is advantageous in its low thickness and high thermal conductivity. Compared with copper foil, aluminum foil is advantageous in its low modulus and small thickness, but it is disadvantageous in its low thermal conductivity. Compared with both copper and aluminum foils, flexible graphite is disadvantageous in its large thickness and low thermal conductivity, but it is advantageous in its low modulus. Indium foil has the best overall combination of properties, as shown by its best performance among the four types of sheet at 0.69 MPa for both the rough and smooth cases. The superiority of indium is due to its lower modulus compared with copper and aluminum foils and higher thermal conductivity compared with flexible graphite.

In the smooth case, the TCCs of coated aluminum, indium, and coated copper foil are close and higher than that of coated flexible graphite. This is because the low roughness and consequent large contact area make flexible graphite's advantageous low modulus less influential.

Figure 6 shows TCCs for the thickness range of 1 μm to 400 μm for the rough case. Figure 7 shows TCCs for the thickness range of 1 μm to 3000 μm for the smooth case. The part of Fig. 7 which is related to the thickness range of 1 μm to 130 μm is magnified in Fig. 8. According to these graphs, coated copper foil and coated flexible graphite show, respectively, the least and the most increase in TCC with decreasing thickness. This is due to the high thermal conductivity of copper and the low thermal conductivity of

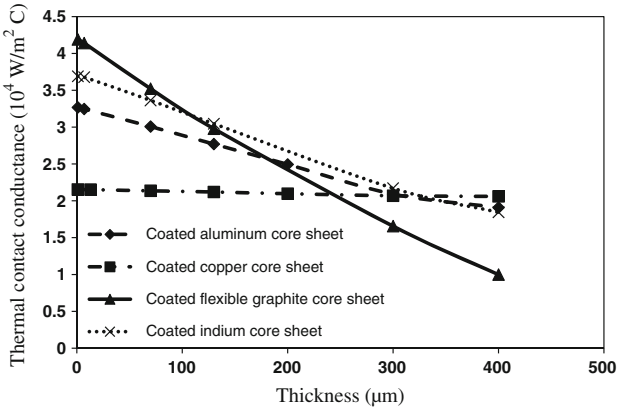

Fig. 6. Effect of core sheet thickness on the thermal contact conductance (TCC) for the four types of core sheet in the case of rough proximate surfaces. Thickness range: 1 μm to 400 μm.

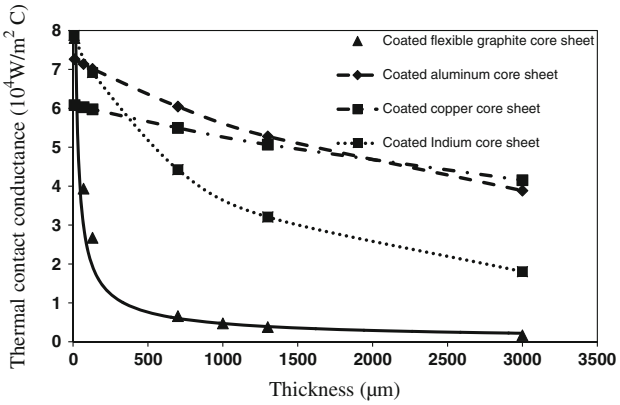

Fig. 7. Effect of core sheet thickness on the thermal contact conductance (TCC) for the four types of coated sheet in the case of smooth proximate surfaces. Thickness range: 1 μm to 3000 μm.

flexible graphite. Flexible graphite and indium have the best performance in both the rough and smooth cases when the foil thickness is very low. This is in agreement with a prior report[13] that carbon black paste with lower thickness (due to higher spreadability) has a much higher TCC in the smooth case compared with metal particle paste, in spite of the low thermal conductivity of the carbon black paste.

As shown in Fig. 6, 7, and 8, there is a difference in TCC among the four core sheets when the thickness of the core sheet is near zero (1 μm), in spite of the effect of the thermal conductivity of the core sheet becoming negligible for such a thickness. This result at a core sheet thickness of near zero is due to the difference in interfacial conductance between the paste and core sheet among the various core sheets (Table III).

In comparison of the performance of various pastes, a very low thickness is a disadvantage in the rough case because of the consequent low fractional valley filling, but is an advantage in the smooth case because valleys, which are very small, are filled completely.[13] In comparison of the performance of various core sheets, the change of the fractional

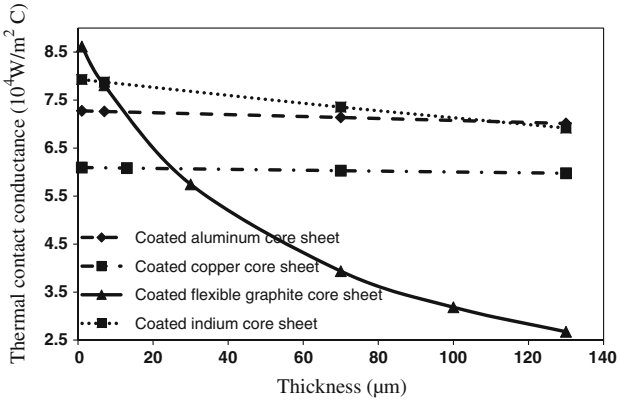

Fig. 8. Effect of core sheet thickness on the thermal contact conductance (TCC) for the four types of coated sheet in the case of smooth proximate surfaces. Thickness range: 1 μm to 130 μm.

valley filling due to a change of the sheet thickness is negligible due to the high modulus of the core sheets compared with the paste. Therefore, a decrease in the core sheet thickness would decrease the length of the heat flow path and thereby increase the TCC in both the rough and smooth cases.

In comparison of the four types of core sheet with identical thickness, as achieved through the modeling, it was found that, in the case of rough proximate surfaces, indium foil gives the best performance in the range of 117 μm to 320 μm foil thickness. For thicknesses below and above this range, flexible graphite and copper foil, respectively, perform the best. In the case of smooth proximate surfaces, indium foil gives the best performance in the range of 6 μm to 112 μm foil thickness, and aluminum foil gives the best performance in the range of 112 μm to 2000 μm foil thickness. For thicknesses below and above this range, flexible graphite and copper foil, respectively, perform the best.

In this work, carbon black paste is the only paste that is modeled. Considering the results of our previous work,[13] TCCs for core sheets coated with metal particle paste may be predicted to be lower than the values in Table IV for carbon black paste. However, the relative performance of TIMs with various core sheets is not expected to change substantially when metal particle paste is used in place of carbon black paste.

CONCLUSIONS

The performance of thermal interface materials in the form of thermal-paste-coated sheets is numerically modeled by finite-element analysis, using ANSYS software. The paste is polyol-ester-based carbon black paste. Four types of core sheet are evaluated, namely copper foil, aluminum foil, indium foil, and flexible graphite. Flexible graphite is advantageous in its resiliency and low modulus, while the metals are advantageous in their high

thermal conductivity and small thickness. Among the three metals, indium has the lowest modulus and the lowest thermal conductivity. The experimental results for comparison with the modeling results were obtained in prior work[3] by sandwiching each coated sheet between two copper blocks at controlled pressure. The surface of each copper block has controlled roughness, such that two levels of roughness are evaluated. Good agreement is found between the modeling and experimental results.

Among the four types of core sheet with identical thickness, coated indium foil gives the best performance for the range of core sheet thickness of 6 μm to 112 μm for the case of smooth (0.01 μm roughness) proximate surfaces and 117 μm to 320 μm for the case of rough (15 μm roughness) proximate surfaces. Aluminum foil gives the best performance for the core sheet thickness range of 112 μm to 2000 μm. For thicknesses below these ranges, flexible graphite performs the best. For thicknesses above these ranges, copper foil performs the best.

REFERENCES

1. C. Lin and D.D.L. Chung, *J. Mater. Sci.* 42, 9245 (2007).
2. C. Lin and D.D.L. Chung, *Carbon* 45, 2922 (2007).
3. C. Leong, Y. Aoyagi, and D.D.L. Chung, *Carbon* 44, 435 (2006).
4. C. Leong, Y. Aoyagi, and D.D.L. Chung, *J. Electron. Mater.* 34, 1336 (2005).
5. C. Leong and D.D.L. Chung, *Carbon* 42, 2323 (2004).
6. C. Leong and D.D.L. Chung, *Carbon* 41, 2459 (2003).
7. C. Lin, T.A. Howe, and D.D.L. Chung, *J. Electron. Mater.* 36, 659 (2007).
8. T.A. Howe, C.-K. Leong, and D.D.L. Chung, *J. Electron. Mater.* 35, 1628 (2006).
9. Y. Xu, C. Leong, and D.D.L. Chung, *J. Electron. Mater.* 36, 1181 (2007).
10. H. Huang, C. Liu, Y. Wu, and S. Fan, *Adv. Mater.* 17, 1652 (2005).
11. C. Lin and D.D.L. Chung, *J. Electron. Mater.* 37, 1698 (2008).
12. A. Yu, P. Ramesh, M.E. Itkis, E. Bekyarova, and R.C. Haddon, *J. Phys. Chem. C* 111, 7565 (2007).
13. P.P.S.S. Abadi, C.-K. Leong, and D.D.L. Chung, *J. Electron. Mater.* 38, 175 (2009).
14. R. Prasher, *Proc. IEEE* 94, 1571 (2006).
15. E.E. Marotta, S.J. Mazzuca, and J. Norley, *IEEE Trans. Compon. Packag. Tech.* 28, 102 (2005).
16. S. Shaikh, K. Lafdi, and E. Silverman, *Carbon* 45, 695 (2007).
17. C.-P. Chiu, G.L. Solbrekken, and Y.D. Chung, *Proceedings of the 13th IEEE Semiconductor Thermal Management and Management Symp*. (Institute of Electrical and Electronics Engineers, 1997), p. 57.
18. R.A. Shaik, A.N. Beall, and A. Razani, *Heat Transfer Eng.* 22, 41 (2001).
19. K. Zhang, M.M.F. Yuen, N. Wang, J.Y. Miao, D.G.W. Xiao, and H.B. Fan, *Proc. 56th Electronic Components and Technology Conf.* (San Diego, CA, 2006), p. 177.
20. R. Schacht, D. May, B. Wunderle, O. Wittler, A. Gollhardt, B. Michel, and H. Reichl, *Proc. 12th Therminic 2006* (Nice, Côte d'Azur, France, 2006).
21. D.D.L. Chung, *J. Mater. Sci.* 39, 2645 (2004).
22. R.L. Webb and J.P. Gwinn, *Proc. ITherm* (2002), p. 671.
23. F. Hua, C. Deppisch, and T. Fitzgerald, *Adv. Microelectron*. 16 (2006).
24. M.G. Cooper, B.B. Mike, and M.M. Yovanovich, *Int. J. Heat Mass Trans.* 12, 279 (1969).
25. J.A. Greenwood and J.B.P. Williamson, *Proc. R. Soc. Lond. A* 295, 300 (1966).
26. C. Lin and D.D.L. Chung, *Carbon* 47, 295 (2009).
27. A. Buch, *Short Handbook of Metal Elements Properties and Elastic Properties of Pure Metals* (Warsaw: Krzysztof Biesaga, 2005), pp. 35–42.
28. I. Michio and F.Y. Kang, *Carbon Materials Science and Engineering—From Fundamentals to Applications* (Beijing: Tsinghua University Press, 2006), p. 335.